Adaptive Piezoelectric Shunt Damping

A. J. Fleming* S. O. R. Moheimani
School of Electrical Engineering and Computer Science
University of Newcastle NSW 2308 Australia

ABSTRACT

Piezoelectric shunt damping systems reduce structural vibration by shunting an attached piezoelectric transducer with an electrical impedance. Current impedance designs result in a coupled electrical resonance at the target modal frequencies. In practical situations, variation in structural load or environmental conditions can result in significant changes in the structural resonance frequencies. This variation can severly reduce shunt damping performance as the electrical impedance remains tuned to the nominal resonance frequencies. This paper introduces a method for online adaption of the shunting impedance. A reconstructed estimate of the RMS strain is minimized by varying the component values of a synthetic shunt damping circuit. The presented techniques are applied in real time, to tune the component values of a randomly excited beam.

1. INTRODUCTION

Piezoelectric transducers (PZT's) in conjunction with appropriate circuitry, can be used as a mechanical energy dissipation device. If a simple resistor is placed across the terminals of the PZT, the PZT will act as a viscoelastic damper[1] . If the network consists of a series inductor-resistor $R-L$ circuit, the passive network combined with the inherent capacitance of the PZT creates a damped electrical resonance. The resonance can be tuned so that the PZT acts as a tuned vibrational energy absorber[1] . Wu[2] reports a method for damping multiple vibration modes with a single PZT. The circuit requires as many $R-L$ parallel branches as there are modes to be controlled. Each branch also contains "current blocking" networks, each consisting of an inductor and capacitor connected in parallel to isolate adjacent branches. Passive shunt damping is regarded as a simple, low cost, light weight, and easy to implement method of controlling structural vibrations.

In practical situations, variation in structural load or environmental conditions can result in significant movement of the structural resonance frequencies. Such variation can severely reduce shunt damping performance as the electrical impedance remains tuned to the nominal resonance frequencies. This problem was first addressed by Smith, Maly, and Johnson[3] , where a viscoelastic spring, with temperature dependant stiffness, was used as a tuned mechanical absorber. Hollkamp[4] later proposed a similar methodology for piezoelectric shunt damping. A mechanically driven resistor was used to vary the virtual inductance of a single mode shunt damping circuit. The performance function, related to the RMS strain, was estimated using an additional piezoelectric patch. In this paper we consider the effect of broadband disturbances on structures with multiple high profile modes. Another approach based on capacitive shunting, considers tonal disturbances and structures with a single dominant lightly damped mode[5] . In situations involving non-sinusoidal disturbances, such techniques are deemed undesirable as the structural response is increased outside of the damped region.

Recently, a new method for implementing shunt damping circuits has been introduced. The *synthetic impedance*[6–8] , uses a voltage controlled current source and DSP system to implement the terminal impedance of an arbitrary shunt network. It replaces physical circuits to provide effective structural damping avoiding the problems encountered with direct circuit implementations. Because the desired impedance is now defined only by a transfer function on the DSP system, the component values are easily modified online.

This paper introduces a technique for online adaptation of shunt network component values. A single piezoelectric patch is used to simultaneously damp multiple modes of the mechanical system and to procure an estimate of the performance function. Experimental results are presented for a randomly excited, simply supported beam. The second and third modes of the beam are controlled with an attached piezoelectric

*Corresponding author:- Email: ajf203@alinga.newcastle.edu.au; Phone: +61 2 4921 7223. Web page: Laboratory for Dynamics and Control of Smart Structures, http://rumi.newcastle.edu.au

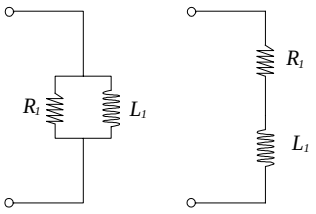

Figure 1: Single mode shunt damping circuits.

transducer and adaptive shunt damping system. The algorithm is shown to regain optimal damping performance after severely detuning the component values.

The paper is presented in six sections. We begin with a brief review of piezoelectric shunt circuit design and a description of the synthetic impedance. In section three we will discuss the modelling of structural dynamics and show how to model the presence of an electrical shunt impedance. The adaptive impedance is introduced in section four. Experimental and theoretical results are presented in section five. We conclude with a review of the initial goals, a summary of the results, and some future directions for research on adaptive shunt damping.

2. PIEZOELECTRIC SHUNT DAMPING

Shunt damping methodologies are often grouped into two broad categories: single mode and multi-mode. Single mode shunt damping techniques are simple but damp only one structural mode for every PZT. Multiple mode shunt damping techniques require more complicated shunt circuits but are capable of damping many modes.

2.1. Single Mode Shunt Damping

Single mode damping was introduced to decrease the magnitude of one structural mode[9] . Two examples of single mode damping are shown in Figure 1, parallel and series shunt damping. The combination of an $R-L$ shunt circuit combined with the intrinsic capacitance of the PZT introduces an electrical resonance. This can be tuned to one structural mode in a manner analogous to a mechanical vibration absorber. Single mode damping can be applied to reduce several structural modes with the use of as many piezoelectric patches and damping circuits.

Problems may result if these piezoelectric patches are bonded to, or imbedded in the structure. First, the structure may not have sufficient room to accommodate all of the patches. Second, the structure may be altered or weakened when the piezoelectric patches are applied. In addition, a large number of patches can increase the structural weight, making it unsuitable for applications such as aerospace.

2.2. Multiple Mode Shunt Damping

To alleviate the problems associated with single mode damping, multi-mode shunt damping has been introduced; i.e. the use of one piezoelectric patch to damp several structural modes. Two multimode shunt damping methodologies will be discussed: Current blocking techniques as presented in[2, 10–12] , and current flowing techniques as presented in[13, 14] .

2.2.1. Current Blocking Techniques

The principle of multi-mode shunt damping is to insert a *current blocking* network[2, 10–12] , in series with each shunt branch. In Figure 2, the blocking circuit consists of a capacitor and inductor in parallel, $C_3 - L_3$. The number of antiresonant circuits in each $R-L$ shunt branch increases with the number of structural modes to be damped simultaneously. Each $R-L$ shunt branch is designed to damp one structural mode. For example, $R_1 - L_1$ in Figure 2 is tuned to resonate at ω_1, the resonance frequency of the first structural mode to be damped. $R_2 - L_2$ is tuned to ω_2, the second structural mode to be damped, and so on.

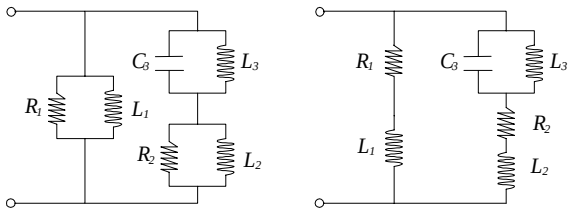

Figure 2: Parallel and series multimode shunt damping circuits.

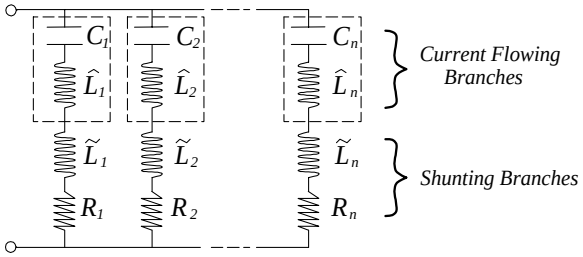

Figure 3: Current flowing piezoelectric shunt damping circuit.[14]

According to Wu[2] , the inductance values for the shunt circuits shown in Figure 2 can be calculated from the following expressions. It is assumed that $\omega_1 < \omega_2$.

$$L_1 = \frac{1}{\omega_1^2 C_p} \quad \tilde{L}_2 = \frac{1}{\omega_2^2 C_p} \quad L_3 = \frac{1}{\omega_1^2 C_3} \quad L_2 = \frac{\left(L_1\tilde{L}_2 + \tilde{L}_2 L_3 - L_1 L_3 - \omega_2^2 L_1 \tilde{L}_2 L_3 C_3\right)}{\left(L_1 - \tilde{L}_2\right)\left(1 - \omega_2^2 L_3 C_3\right)} \tag{1}$$

where C_p is the capacitance of the PZT, and C_3 is an arbitrary capacitor used in the current blocking network.

2.2.2. Current Flowing Techniques

One problem with the previous technique is that the order of the shunt circuit increases quadratically as the number of modes to be shunt damped increases. Current flowing circuits[14] , such as that pictured in Figure 3, are easier to tune and increase in order only linearly as a greater number of modes are to be shunt damped simultaneously.

At a specific frequency ω_i, the inductor capacitor network $C_i - \widehat{L}_i$ allows current to flow through the rest of the branch, at all other frequencies the network appears approximately as an open circuit. The damping inductor and resistor $\widetilde{L}_i - R_i$ act like a single mode shunt circuit at the frequency ω_i. The circuit is simplified by combining the series inductors.

2.3. The Synthetic Impedance

The synthetic impedance[6–8] allows the implementation of complicated multimode shunt damping circuits using only a few opamps, one resistor, and a digital signal processor (DSP).

The synthetic impedance is a two terminal device that establishes an arbitrary relationship between voltage and current at its terminals[7] . The functionality is shown in Figure 4, where $i_z(t) = f(v_z(t))$. This can be made to synthesize any network of physical components by fixing i_z to be the output of a linear transfer function with input v_z. i.e.

$$I_z(s) = Y(s)V_z(s) \tag{2}$$

where $Y(s) \equiv \frac{1}{Z(s)}$ and $Z(s)$ is the impedance to be seen from the terminals.

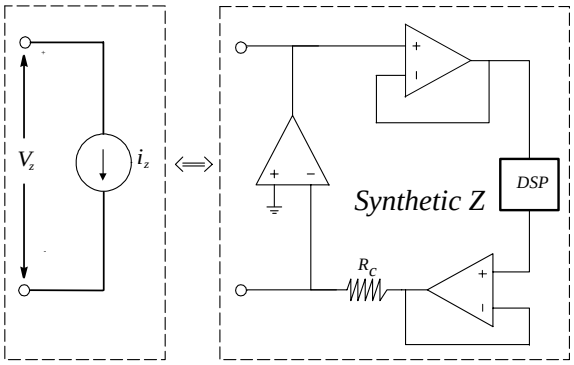

Figure 4: Functionality of the synthetic impedance

3. MODELLING THE COMPOUND SYSTEM

For generality, we will enter the modelling process with knowledge *a priori* of the systems dynamics. As an example we will consider a simply supported beam with two bonded piezoelectric patches, one to be used as a source of disturbance, and the other for shunt damping. The transfer function $G_{vv}(s)$ from applied actuator voltage to sensor voltage can be derived analytically from the Euler-Bernouli beam equation[15] , or obtained experimentally through system identification[16] . Using similar methods, we may obtain the transfer function from applied actuator voltage to displacement at a point $G_{yv}(x,s)$.

Following the modal analysis procedure[17] , the resulting transfer functions have the familiar form.

$$G_{yv}(x,s) \triangleq \frac{Y(x,s)}{V_a(s)} = \sum_{i=1}^{\infty} \frac{F_i \phi_i(x)}{s^2 + 2\zeta_i w_i s + w_i^2} \tag{3}$$

$$G_{vv}(s) \triangleq \frac{V_s(s)}{V_a(s)} = \sum_{i=1}^{\infty} \frac{\alpha_i}{s^2 + 2\zeta_i w_i s + w_i^2}. \tag{4}$$

where $Y(x,s)$ is the measured displacement, $V_s(s)$ is the piezoelectric sensor voltage, and $V_a(s)$ is the voltage applied to a collocated actuator. F_i, and α_i represent the lumped modal and piezoelectric constants applicable to the i^{th} mode of vibration.

The transfer functions of the shunt damped system can be shown to be[18, 19] :

$$\widetilde{G}_{vv}(s) \triangleq \frac{V_s(s)}{V_a(s)} = \frac{G_{vv}(s)}{1 + G_{vv}(s)K(s)}. \tag{5}$$

$$\widetilde{G}_{yv}(x,s) \triangleq \frac{Y(x,s)}{V_a(s)} = \frac{G_{yv}(x,s)}{1 + G_{vv}(s)K(s)}. \tag{6}$$

where

$$K(s) = \frac{Z(s)}{Z(s) + \frac{1}{C_p s}} \tag{7}$$

4. ADAPTIVE SHUNT DAMPING

Before service, shunt circuits are tuned to the structural resonance frequencies of interest. To maintain some kind of optimal performance, we introduce a technique for online tuning of the component values. This technique utilizes the synthetic impedance along with time varying transfer functions to alter the parameters of a shunt circuit in real time.

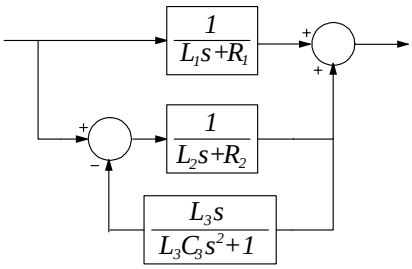

Figure 5: Admittance block diagram of a series two mode shunt damping circuit.

4.1. System Schematic

The damped system transfer function from applied actuator voltage to the measured output V_z is derived in[18]

$$\frac{V_z(s)}{V_a(s)} = \frac{K(s)G_{vv}(s)}{1 + K(s)G_{vv}(s)} \tag{8}$$

Note the output $V_z(s)$ offers little information about the performance of the controller. Traditionally, designers seek to minimize the output magnitude resulting from some disturbance profile. In this case the controller is performing well when there is a lightly damped electrical resonance between the impedance and the piezoelectric transducer at the resonance frequencies. Hence a large measured output can signify a large reduction in structural vibration.

A useful performance signal is the displacement at a point or the equivalent sensor voltage V_s. Both of these quantities are dynamically related to the measured output V_z but are parameterized in terms of the impedance $Z(s)$. This means, to implement an adaptive piezoelectric shunt damping system, we need to synthesize the impedance $Z(s)$ twice. Firstly to implement the shunt damping circuit, and secondly to reconstruct the performance signal V_p.

4.2. Impedance Parameterization

Consider the current blocking multimode shunt circuit shown in Figure 2. This circuit can be parameterized in terms of the branch resistances and resonance frequencies. Unfortunately each branch is not only parameterized in terms of its own resonance frequency but also the resonance frequencies of other branches (due to the current-blockers). The result is an overly complicated expression for each inductor in terms of the desired branch frequencies and can be simplified by explicitly parameterizing the current blocking network and using the results of [7] to generate an equivalent block diagram that can be implemented in real time. Figure 5 shows $Y(s)$ [†], the admittance of a series configuration two mode shunt damping circuit, explicitly broken up into each $R-L$ branch resonance pair and $L-C$ current blocker. The relationship between the parameter vector θ and the component values is shown in (1).

$$\theta = \begin{bmatrix} \omega_1 & \omega_2 & \cdots & \omega_{N_\omega} \end{bmatrix} \tag{9}$$

Alternatively, if a current flowing configuration is to be employed, the components and admittance of each branch can be easily parameterized in terms of the circuits target resonance frequencies[14] . In this case the total admittance of the circuit is simply the sum of a number of second order admittances.

[†] $Y(s)$ is the admittance used to implement $Z(s)$ in the synthetic impedance. Refer to Section 2.3.

4.3. Performance Evaluation

Conventional adaptive feedback control architectures generally make use of a synthesized reference signal to estimate the performance of the controller[20] . An estimate of the nominal sensitivity function $\frac{Y(j\omega)}{D_o(j\omega)}$ is available, where $Y(s)$ is the system output and $D_o(s)$ is the synthesized disturbance. Currently no such method for obtaining an estimate of the disturbance is known. The difficulty is due to the parameterization of the secondary path in the unknown plant we are trying to control. It may be possible to estimate the unknown dynamics of the secondary path on-line (as in [21]), but this is considered an impractical approach to the problem.

4.3.1. The Performance Function

Two performance functions will be presented: The RMS strain $V^{strain}(\theta)$, and the ratio of RMS strain to RMS shunt voltage $V^{ratio}(\theta)$. The former is the obvious choice but is prone to errors due to a dependance on the power of the disturbance, the latter is an approximate method for minimizing the RMS strain, but achieves a degree of isolation from the stochastic characteristics of the disturbance.

RMS Strain The objective will be to minimize $E\left\{V_p(t)^2\right\}$ i.e. to minimize the RMS strain at the piezoelectric transducer ($V_p(t)$ is dynamically proportional to the strain under the piezoelectric patch). The signal $V_p(t)$ can by synthesized in real time from the shunt voltage.[18]

$$\theta^* = \arg\min_{\theta\in\Re^{N_\omega}} V^{strain}(\theta) \tag{10}$$

$$= \arg\min_{\theta\in\Re^{N_\omega}} E\left\{V_p^2(t)\right\} \tag{11}$$

The performance function $V^{strain}(\theta)$ is approximated by its discrete time equivalent

$$V_k^{strain}(\theta) = \frac{1}{N}\sum_{i=kN}^{(k+1)N-1} V_p^2(iT_s) \tag{12}$$

where T_s is the sampling interval and N is the number of samples in each k^{th} record interval.

The disturbance signal must be stationary so that the performance estimates $V_k(\theta), V_{k+1}(\theta), \ldots, V_{k+M}(\theta)$ are consistent and unbiased. We refer to the term stationary as 'wide-sense stationary'[22] relative to N. e.g. stationary over the interval $T_s\left[\begin{array}{cc} kN & (k+M)N-1 \end{array}\right]$.

If V_p is stationary, $V_k(\theta)$ can be shown to be a consistent and unbiased estimator over a single record interval. The requirement for stationarity is extended to M such intervals so that there will be at least M consecutive estimates of $V(\theta)$ with similar disturbance. In practice, the encountered size of M will define the amount of noise and bias in the gradient estimates.

RMS Ratio If the disturbance is not sufficiently stationary, the above performance function will not provide a useful estimate of the damping performance. Consider the model of a disturbance shown in Figure 6, where n_k is a white noise source, $H_n(j\omega)$ is a noise filter, and α is a slowly time varying gain. Although the signal $u(t)$ is not stationary, if the gain α varies sufficiently slowly, the power spectral density of adjacent record intervals will differ only by a constant gain α^2. The aim is to define a performance function independent of α^2.

Consider the performance function (13).

$$V_k^{ratio}(\theta) = \frac{\sum_{i=kN}^{(k+1)N-1} V_p^2(iT_s)}{\sum_{i=kN}^{(k+1)N-1} V_R^2(iT_s)} \tag{13}$$

where V_R is the voltage across the shunting resistor. As both of the impedance structures, current blocking and current flowing, approximate a series inductor and resistor around a specific resonance frequency, we can estimate the signal V_R for each of the shunt branches by filtering the shunt voltage,

$$V_R(s) = V_z(s)\frac{R}{Ls+R} \tag{14}$$

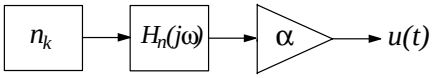

Figure 6: Disturbance noise model.

where L is the inductor value currently being implemented. For multiple modes the performance function can be decomposed into its modal components by appropriately pre-filtering V_z. Intuitively, by minimizing $V_k^{ratio}(\theta)$, we are minimizing the RMS strain, and maximizing the voltage across the shunting resistance. Maximizing the voltage across a shunt resistance will maximize the amount of dissipated energy. For any given disturbance, both the numerator and denominator are linear in α^2, hence, the performance function is independent of the excitation level α.

4.3.2. Typical Performance Curves

Because of the analytic complexity of the performance functions, little is known of their properties. By simulation, both are insensitive to reasonable changes in damping ratio, but as expected, are strong functions of the branch resonance frequencies.

RMS Strain The surface is definitely not convex but appears to have a single global minima.The performance function is plotted against the resonance frequency of the second mode in Figure 7 a). Over a certain modal frequency range the contribution from adjacent modes is small, allowing the performance function to be uncoupled into its modal components.

RMS Ratio The RMS ratio performance function is plotted in Figure 7 a). As with the previous case, the function is non-convex but appears to have a single global minima. It should be noted that the minima of this function does not occur exactly at the minimum of RMS strain (in our case the approximation is correct to 0.01 Hz).

Hollkamp[4] , suggests a performance function similar to (13) with the exceptions: V_p is measured directly from an additional piezoelectric patch, and the denominator is the RMS value of V_z. Figures 7 c) and 7 d) compare the RMS values of V_R and V_z. It can be seen that maximizing the RMS value of V_R is much more desirable than performing the same operation on V_z. These simulations were performed using damping ratios of $\varsigma = 0.005$ for each mode. As the damping ratios are increased, the approximation made by Hollkamp becomes more accurate, i.e. $\arg\max_{\theta \in \Re^{N_\omega}} E\left\{V_z^2(t)\right\}$ approaches $\arg\max_{\theta \in \Re^{N_\omega}} E\left\{V_r^2(t)\right\}$ as the structural damping ratios are increased.

4.3.3. Convergence

For some desired variance in $V_k(\theta)$ it is desirable to estimate the required length of the averaging interval. A large conservative N will result in a small variance but slow update rate. The opposite is true for an insufficiently small N, fast update but large variance. A full discussion on the convergence of the performance functions is provided in.[18] Approximately 35 seconds of data is required to procure an estimate of the performance function for the first three modes of a simply supported beam similar to that discribed in Section 5.1 and [18] .

4.4. Searching the Performance Surface

Given that an estimate of the performance function is available, the parameter vector θ can be updated using a gradient search algorithm. Newton's method[21] is selected for its fast convergence.

$$\theta_{k+1} = \frac{V(\theta_k)(\theta_k - \theta_{k-1})}{V(\theta_k) - V(\theta_{k-1})}. \tag{15}$$

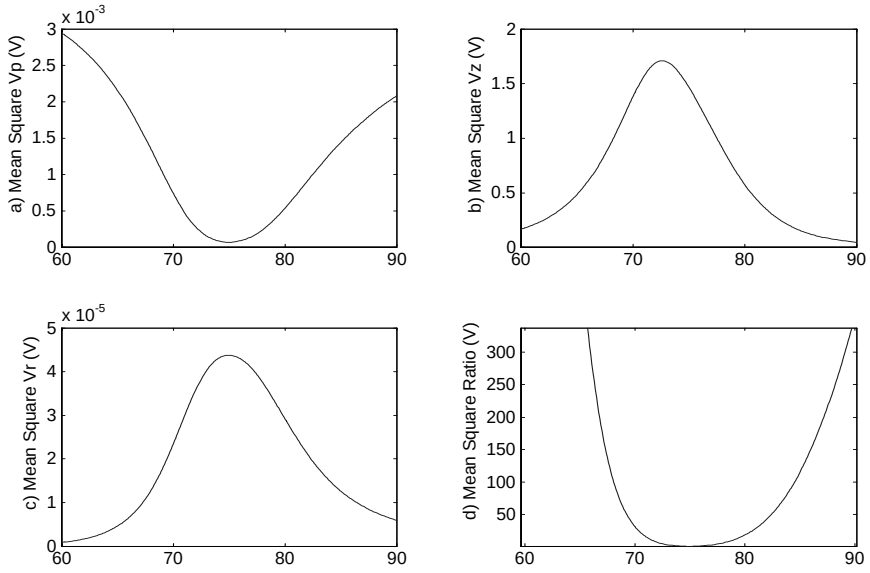

Figure 7: The performance functions plotted against the resonance frequency of the structure in Hz.

Length, L	$0.6\ m$
Width, w_b	$0.05\ m$
Thickness, h_b	$0.003\ m$
Youngs Modulus, E_b	$65 \times 10^9\ N/m^2$
Density, ρ	$2650\ kg/m^2$

Table 1: Experimental Beam Parameters.

For practical reasons the step size is artificially limited. Although this slows convergence, it provides needed robustness to gradient errors and numerical sensitivity at the minima. The real time implementation of the limited Newton search algorithm also contains a small artificial bias to maintain the algorithm if $\theta_k - \theta_{k-1} \approx 0$.

5. EXPERIMENTAL RESULTS

5.1. Experimental Setup

The experimental beam is a uniform aluminum bar with rectangular cross section and experimentally pinned boundary conditions at both ends. A pair of piezoelectric ceramic patches (PIC151) are attached symmetrically to either side of the beam surface. One patch is used as an actuator and the other as a shunting layer. Physical parameters of the experimental beam and piezoelectric transducers are summarized in Tables 1 and 2. Note that the location of the piezoelectric patch offers little control authority over the first mode. In this work, the structure's second and third modes are targeted for reduction.

The displacement and voltage frequency responses are measured using a Polytec laser vibrometer (PSV-300) and a HP spectrum analyzer (35670A).

The current source and buffer/amplifiers required for the synthetic impedance are constructed from Burr Brown OPA445 opamps. These opamps have a supply voltage limit of $\pm 45\ v$. If necessary, the circuit can be constructed from high voltage opamps with supplies of greater than $\pm 400\ V$.

5.2. Damping Performance

To verify the function of the adaptive impedance a poorly tuned shunt circuit is applied to the experimental beam, this is equivalent to a large step change in the resonance frequencies of the structure. It is expected that

Length	$0.070\ m$
Charge Constant, d_{31}	$-210 \times 10^{-12}\ m/V$
Voltage Constant, g_{31}	$-11.5 \times 10^{-3}\ Vm/N$
Coupling Coefficient, k_{31}	0.340
Capacitance, C_p	$0.105\ \mu F$
Width, $w_s\ w_a$	$0.025\ m$
Thickness, $h_s\ h_a$	$0.25 \times 10^{-3}\ m$
Youngs Modulus, $E_s\ E_a$	$63 \times 10^{9}\ N/m^2$
Distance from Beam End	$0.05\ m$

Table 2: Piezoelectric Transducer Properties.

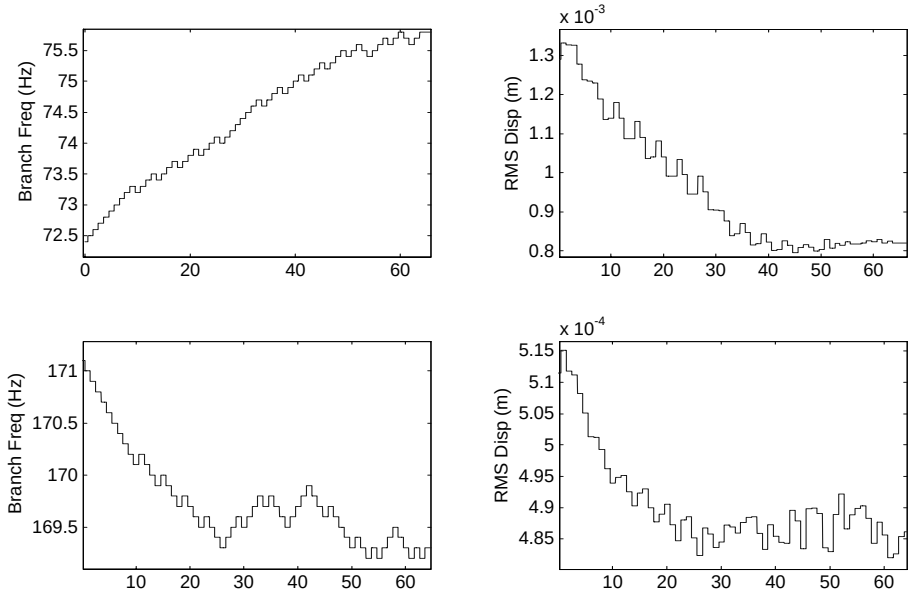

Figure 8. RMS Strain. Experimental evolution of the second and third mode branch frequencies and modal performance components.

the update algorithm will iteratively retune the parameters to minimize (12). In order to perform simulations, a frequency domain subspace algorithm[23,24] is employed to obtain a 10^{th} order model for the two open loop system transfer functions $G_{yv}(s)|_{x=0.17m}$ and $G_{vv}(s)$. The excitation is a pseudo-random signal with fourth order low pass cutoff at 400 Hz.

5.2.1. Performance function: RMS Strain

A parameterized current blocking shunt circuit is applied to the beam. The evolution of the frequency tuned parameters and the RMS displacement for each mode is shown in Figure 8.

5.2.2. Performance Function: RMS Ratio

A parameterized current flowing shunt circuit is applied to the beam. The evolution of the frequency tuned parameters and the performance component of each mode is shown below in Figure 9.

Because of the low gradients around the minima of this performance function, the resonance frequencies tend to drift slightly after adjustment. The low gradients cause the differences in consecutive updates of the performance function to be small over an attributable range of frequencies around the minima, see Figure 9. Figure 10 shows the initial, adapted, and misadjusted displacement frequency responses of the beam. The frequency response c) corresponds to the instance of peak misadjustment in the second mode branch frequency.

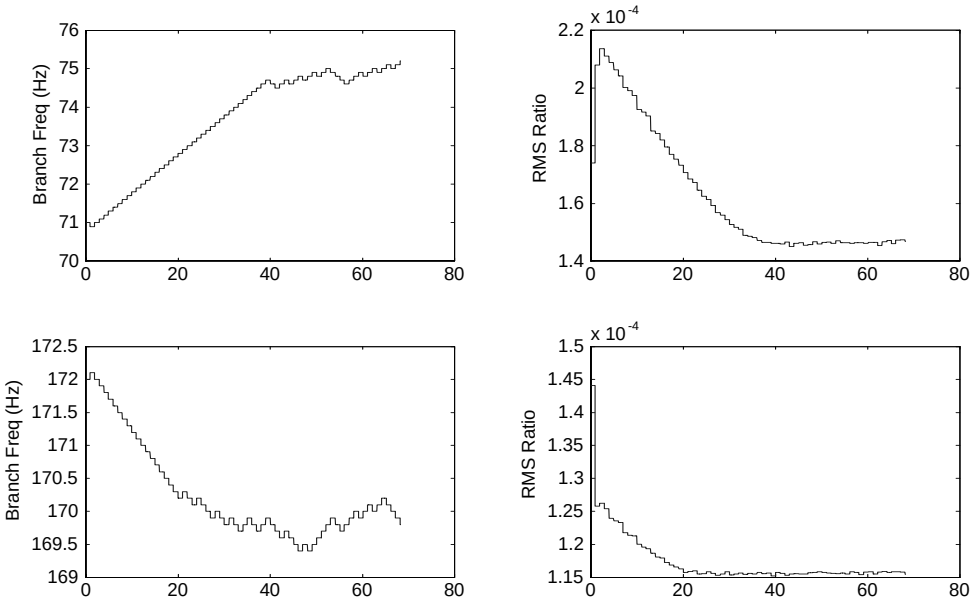

Figure 9. RMS Ratio. Experimental evolution of the second and third mode branch frequencies and modal performance components

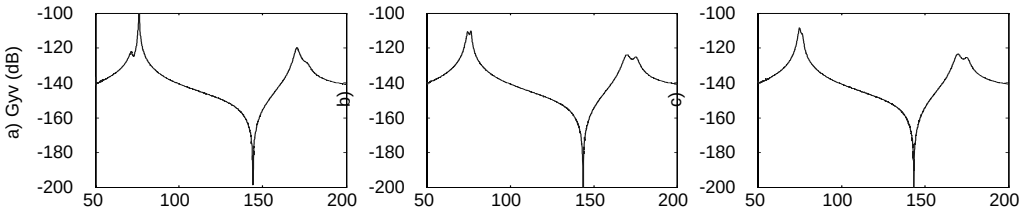

Figure 10. The measured transfer functions from applied voltage to structural displacement ($x = 0.17m$). a) Untuned, b) At the minima, c) Peak misadjustment.

6. CONCLUSIONS

The performance of finely tuned piezoelectric shunt damping systems is extremely sensitive to the resonance frequencies of the host structure. The adaptive impedance allows us to retain the desirable characteristics of shunt damping systems e.g. robustness, while automating the process of component tuning. The presented technique requires only a single patch. An understanding of the underlying feedback structure has allowed us to synthesize additional signals required for adaption. Previously these signals have been obtained from additional patches or accelerometers.

Two performance functions have been proposed:

- The RMS Strain. By synthesizing the piezoelectric sensor voltage, it is possible to estimate the RMS strain under the piezoelectric transducer. This performance function provides reliable tuning only if the disturbance is wide sense stationary. By simulation, the performance function appears to have a single global minima and can be minimized using the Newton search algorithm.
- The RMS Ratio. Minimizing this performance function has the effect of minimizing the synthesized piezoelectric sensor voltage and maximizing the synthesized voltage across the shunting resistances. By simulation, it has a single global minima very close to the minima of the RMS strain. This function is independent of slow variations in the disturbance magnitude.

Experimental results show reliable estimation of the performance functions, optimal tuning of the circuit parameters, and satisfactory misadjustment. The synthetic impedance provides a near ideal means for implementing the shunt circuits, the second and third modes are reduced in magnitude by up to 22 and 19 dB. Although both shunt circuit configurations (current blocking and current flowing) provide similar performance, the current flowing technique requires a lower order admittance transfer function, and is easily parameterized in terms of the branch resonance frequencies. These reasons make the current flowing technique an ideal candidate for damping a large number of modes, as performed in [14] .

Future work on the proposed adaptive scheme may involve a full analysis of the convergence properties. An attempt could also be made to estimate the disturbance, this appears difficult as the secondary path is a strong function of the parameter vector θ. It may also be possible, using small samples of open loop operation, to estimate the resonance frequencies and damping ratios of each mode. If so, the optimal circuit parameters may be estimated in a single update period.

REFERENCES

1. N. W. Hagood and A. Von Flotow, "Damping of structural vibrations with piezoelectric materials and passive electrical networks," *Journal of Sound and Vibration* **146**(2), pp. 243–268, 1991.
2. S. Y. Wu, "Method for multiple mode shunt damping of structural vibration using a single PZT transducer," in *Proc. SPIE Smart Structures and Materials, Smart Structures and Intelligent Systems, SPIE Vol.3327*, pp. 159–168, (Huntington Beach, CA), March 1998.
3. K. E. Smith, J. R. Maly, and C. D. Johnson, "Smart tuned mass dampers," in *Proc. ADPA/AIAA/ASME/SPIE Conference on Active Materials and Adaptive Structures*, pp. 19–22, (Alexandria, VA), 1991.
4. J. J. Hollkamp and T. F. Starchville. Jr., "A self-tuning peizoelectric vibration absorber," *Journal of Intelligent Material Systems and Structures* **5**, pp. 559–565, July 1994.
5. C. L. Davis and G. A. Lesieutre, "An actively tuned solid-state vibration absorber using capacitive shunting of piezoelectric stiffness.," *Journal of Sound and Vibration* **232**, pp. 601–617, May 2000.
6. A. J. Fleming, S. Behrens, and S. O. R. Moheimani, "Synthetic impedance for implementation of piezoelectric shunt-damping circuits," *Electronics Letters* **36**, pp. 1525–1526, August 2000.
7. A. J. Fleming, S. Behrens, and S. Moheimani, "Innovations in piezoelectric shunt damping," in *Proc. SPIE: Symposium on Smart Materials and MEM's, Smart Structures Amd Devices, SPIE Vol.4326*, (Melbourne, Australia), December 2000.

8. A. J. Fleming, S. Behrens, and S. O. R. Moheimani, "Optimization and implementation of multi-mode piezoelectric shunt damping systems," *IEEE/ASME Transactions on Mechatronics* , To be published March 2002.
9. N. W. Hagood and E. F. Crawley, "Experimental investigation of passive enhancement of damping for space structures," *Journal of Guidance, Control and Dynamics* **14**(6), pp. 1100–1109, 1991.
10. S. Y. Wu, "Piezoelectric shunts with parallel R-L circuit for structural damping and vibration control," in *Proc. SPIE Smart Structures and Materials, Passive Damping and Isolation, SPIE Vol.2720*, pp. 259–269, March 1996.
11. S. Y. Wu, "Multiple PZT transducers implemented with multiple-mode piezoelectric shunting for passive vibration damping," in *Proc. SPIE Smart Structures and Materials, Passive Damping and Isolation, SPIE Vol.3672*, pp. 112–122, (Huntington Beach, CA), March 1999.
12. S. Y. Wu and A. S. Bicos, "Structural vibration damping experiments using improved piezoelectric shunts," in *Proc. SPIE Smart Structures and Materials, Passive Damping and Isolation, SPIE Vol.3045*, pp. 40–50, March 1997.
13. S. Behrens, S. O. R. Moheimani, and A. J. Fleming, "Multiple mode current flowing passive piezoelectric shunt controller," *Journal of Sound and Vibration* , Submitted January 2002.
14. S. Behrens and S. O. R. Moheimani, "Current flowing multiple mode piezoelectric shunt dampener," in *Proc. SPIE Smart Materials and Structures, Paper No. 4697-24*, (San Diego, CA), March 2002.
15. C. R. Fuller, S. J. Elliott, and P. A. Nelson, *Active Control of Vibration*, Academic Press, 1996.
16. L. Ljung, *System Identification: Theory for the User*, Prentice Hall, 1999.
17. L. Meirovitch, *Elements of Vibration Analysis*, McGraw-Hill, Sydney, 2nd ed., 1996.
18. A. J. Fleming and S. O. R. Moheimani, "Adaptive piezoelectric shunt damping," *Smart Materials and Structures* , Scheduled for publication 2002.
19. S. O. R. Moheimani, A. J. Fleming, and S. Behrens, "On the feedback structure of wideband piezoelectric shunt damping systems," *Smart Materials and Structures* , Accepted for publication 2002.
20. S. M. Kuo and D. R. Morgan, *Active Noise Control Systems*, Wiley, 1996.
21. B. Widrow and S. D. Stearns, *Adaptive Signal Processing*, Prentice Hall, Signal Processing Series, 1985.
22. R. G. Brown and P. Hwang, *Introduction to Random Signals and Applied Kalman Filtering*, ch. 2.4. John Wiley and Sons Inc., 1997.
23. T. Mckelvy, H. Akcay, and L. Ljung, "Subspace based multivariable system identification from frequency response data," *IEEE Transactions on Automatic Control* **41**, pp. 960–978, July 1996.
24. T. McKelvey, A. J. Fleming, and S. O. R. Moheimani, "Subspace based system identification for an acoustic enclosure," *ASME Jounrnal of Vibration and Acoustics* , Scheduled for Publication 2002.